ATMOSPHERIC SCIENCE

Mechanisms and competition of halide substitution and hydrolysis in reactions of N_2O_5 with seawater

Laura M. McCaslin[1], Mark A. Johnson[2], R. Benny Gerber[1,3]*

S_N2-type halide substitution and hydrolysis are two of the most ubiquitous reactions in chemistry. The interplay between these processes is fundamental in atmospheric chemistry through reactions of N_2O_5 and seawater. N_2O_5 plays a major role in regulating levels of O_3, OH, NO_x, and CH_4. While the reactions of N_2O_5 and seawater are of central importance, little is known about their mechanisms. Of interest is the activation of Cl in seawater by the formation of gaseous $ClNO_2$, which occurs despite the fact that hydrolysis (to HNO_3) is energetically more favorable. We determine key features of the reaction landscape that account for this behavior in a theoretical study of the cluster $N_2O_5/Cl^-/H_2O$. This was carried out using ab initio molecular dynamics to determine reaction pathways, structures, and time scales. While hydrolysis of N_2O_5 occurs in the absence of Cl^-, results here reveal that a low-lying pathway featuring halide substitution intermediates enhances hydrolysis.

INTRODUCTION

Hydrolysis and S_N2-type halide substitution reactions are two ubiquitous families of reactions that are important throughout many disciplines of chemistry. One area in which the interplay of these key processes has major implications in heterogeneous atmospheric chemistry is the reactions of N_2O_5 with seawater and halide-containing sea spray aerosols. The reactive uptake of N_2O_5 on sea spray aerosols is widely believed to be the most influential set of reactions in heterogeneous atmospheric chemistry (*1*–*7*). Model studies indicate that changes in the probability of the reactive uptake of N_2O_5 on aerosols change atmospheric levels of NO_x, O_3, and OH by up to 25, 12, and 15%, respectively (*2*). N_2O_5 is formed from NO_2 and NO_3 during the night, as NO_3 is photolyzed by sunlight. HNO_3, the hydrolysis product of N_2O_5 reactions with seawater, serves as a major sink for NO_x species in the atmosphere, which has been validated by a variety of modeling and field studies (*1*, *2*, *7*–*11*). NO_x species are widely known to affect levels of O_3, OH, and CH_4, thus motivating the need to study their formation and depletion pathways (*12*). Studies have also shown formation of $ClNO_2$ from N_2O_5 interacting with chloride-containing liquids, aerosols, and small water clusters (*7*, *13*–*16*) in a wide range of chloride concentrations. These $ClNO_2$ compounds can photolyze to form NO_2 and chlorine radicals, which is a major source of activated Cl in the atmosphere (*17*, *18*). The competition between formation of $ClNO_2$ from halide substitution reactions and HNO_3 from hydrolysis reactions of N_2O_5 and seawater thus has major consequences for the fate of NO_x species, CH_4, and O_3, which are known to greatly affect Earth's radiative forcing and thus global climate (*19*).

Recently, experiments on both liquid surfaces and aerosols have been performed to unravel the competition between numerous reaction pathways when N_2O_5 interacts with seawater and sea spray aerosols (*20*–*23*). Limits on the total reactive uptake of N_2O_5 on both pure and salty water have been determined to be between 0.01 and 0.03. However, due to the complexity of chemical environments of sea spray aerosols, studies of the relative yields of $ClNO_2$ and HNO_3 are still under way (*15*, *24*, *25*). While some theoretical studies have explored hydrolysis and halide substitution of N_2O_5 interacting with small water clusters, mechanisms of the competition between these reactions have yet to be established (*16*, *26*–*33*).

Faced with the need to understand these complex reactions and their mutual influence on each other, it is necessary to design model systems that help to develop intuition from first-principles studies. In this work, we seek to reveal intrinsic features of the reaction between N_2O_5 and aqueous Cl^- that control the competition between hydrolysis and halide substitution reactions. We specifically address how water competes with Cl^- for reaction with N_2O_5 in a theoretical study of the ternary ionic cluster with composition $N_2O_5/Cl^-/H_2O$. Scrutiny of this microscopic regime is also warranted by the results of a recent mass spectrometric experimental study of N_2O_5 interactions with small halide-water clusters $[X^-(H_2O)_{n=1-5}]$. (*16*). Intermediates were isolated and characterized with infrared spectroscopy to reveal formation of XNO_2/NO_3^- species with composition $X^-(N_2O_5)$. In the present work, we address the features in the reaction dynamics that control the competition between halide substitution and hydrolysis in a sufficiently small system that it can be studied using very accurate ab initio methods. In studying the reaction pathways and time scales of these processes, insights will be gained into the microscopic details of unresolved questions in heterogeneous atmospheric chemistry. Our method integrates the calculations of transition states (TSs), intrinsic reaction coordinates (IRCs), and ab initio molecular dynamics (AIMD). An additional strength of this small model is its ability to evaluate how mechanistic details for the reactions of N_2O_5 with aqueous chloride will evolve in larger systems. We take the perspective that even in bulk environments, the chemistry of halide substitution and hydrolysis of N_2O_5 is likely a local phenomenon. Thus, even as the addition of water molecules to the system will inevitably change the rates of the processes because of a decrease in accessibility of the TS, the configurations and relative energies of the TS will be preserved and continue to provide a microscopic paradigm for the overall kinetics.

[1]Institute of Chemistry and the Fritz Haber Center for Molecular Dynamics, The Hebrew University, Jerusalem 9190401, Israel. [2]Department of Chemistry, Yale University, New Haven, CT 06525, USA. [3]Department of Chemistry, University of California, Irvine, Irvine, CA 92697, USA.
*Corresponding author. Email: benny@fh.huji.ac.il

RESULTS AND DISCUSSION

Figure 1 represents the reaction pathway for N_2O_5 interacting with H_2O and Cl^-. Solid lines connecting the various structures indicate an IRC, the steepest gradient pathway from a TS to nearest local minimum (*34*). Here, two TSs and thus two IRCs are indicated. First, the left IRC corresponds to the pathway from Cl^-/H_2O interacting with intact N_2O_5 through an extremely small barrier (0.6 kcal/mol) into the formation of substitution products: $ClNO_2$, NO_3^-, and H_2O. This small barrier to substitution and small distance in configuration space between the reactant and TS1 structures implies a very fast process. Within the substitution product region (i.e., configurations of $ClNO_2/NO_3^-/H_2O$), there is a rich array of configurations accessible to the system at ambient temperatures due to the electrostatically bound nature of the ternary cluster. Besides the local minima associated with IRCs, an additional minimum is indicated: a planar conformation of $ClNO_2/NO_3^-/H_2O$. The planar $ClNO_2/NO_3^-$ substructure has the same orientation as the reaction intermediate recently detected by Kelleher *et al.* (*16*). As Kelleher *et al.* found, this structure with a relative energy of 15.6 kcal/mol has the lowest energy of the substitution products. The third substitution structure shown in Fig. 1 (differing in orientation and number of hydrogen bonds) has a relative energy of 21.1 kcal/mol and connects to the second IRC shown in Fig. 1, linking substitution and hydrolysis reactions (i.e., configurations of $HNO_3/NO_3^-/HCl$ or $2HNO_3/Cl^-$). The TS with relative energy of 35.5 kcal/mol connecting the substitution and hydrolysis product regions (TS2) exhibits the interesting structural feature that the charge-separated NO_2^+ and NO_3^- moieties accommodate Cl^- and H_2O on opposite sides of the NO_2^+ constituent such that both nucleophiles are positioned to attack the nitrogen atom. This configuration illustrates the mutual influence of the halide substitution and hydrolysis reactions of N_2O_5, indicating that the conditions for one reaction necessarily affect the other. On the right side of the second IRC, a structure corresponding to a hydrolysis reaction sits at 0.0 kcal/mol, the lowest-lying structure found. This $HCl/NO_3^-/HNO_3$ structure is 15.6 kcal/mol and 30.4 kcal/mol more stable than the lowest-lying substitution and intact N_2O_5 configurations, respectively. Both O—H bonds of the water have broken, and the protons have formed new bonds to make HCl and HNO_3. Last, another low-lying minimum structure of $2HNO_3/Cl^-$ is shown to the far right at 0.4 kcal/mol.

Thermodynamically, the trends in the potential energy surface are clear: Hydrolysis products are by far the most stable species, although substitution products are more stable than intact $N_2O_5/Cl^-/H_2O$ by 9.3 to 14.8 kcal/mol. The stability of the hydrolysis products fits the current model of HNO_3 as a sink for NO_x species (*2*, *35*, *36*). We note that $ClNO_2$ production is found to exceed that of HNO_3 in most media, although the relative yields of these species need further investigation (*20*, *22*, *37*). Analogous studies of the hydrolysis reaction of N_2O_5 with two water molecules (where a second H_2O replaces Cl^- in our system) determine the barrier to reaction from the associated $N_2O_5/2H_2O$ cluster to be ~20 kcal/mol (*24*). Here, the difference between the low-lying isomer of N_2O_5 at 30.4 kcal/mol (Fig. 1) and the TS to hydrolysis (TS2) at 41.3 kcal/mol (Fig. 1) is a mere 5.1 kcal/mol. Despite this ~15 kcal/mol lowering of the barrier to N_2O_5 hydrolysis in the presence of Cl^-, the addition of a third body adds entropic complexity. The presence of Cl^-, as opposed to another water molecule, near NO_2^+ stabilizes the hydrolysis process by removing a proton from the water, lowering the barrier to hydrolysis. While the hydrolysis process is thermodynamically favored, the substitution process occurs much more quickly because of its low barrier. The heights of the barriers are correlated with the configurational distance between reactants and products. Because the TS of the halide substitution process (TS1) is very close in configuration to the intact $N_2O_5/Cl^-/H_2O$ minimum, the barrier is quite small (0.6 kcal/mol). Despite the close proximity of the attacking water to NO_2^+ in TS2, the system must undergo a much greater change in geometry between the adjacent $ClNO_2/H_2O/NO_3^-$ minimum and charge-separated TS structure, resulting in a much higher barrier (14.4 kcal/mol).

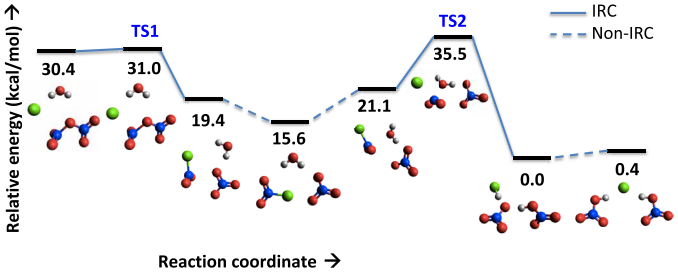

Fig. 1. Low-lying reaction pathway of N_2O_5 interacting with $H_2O + Cl^-$. Structures were optimized at the ωB97X-D/aug-cc-pVDZ level of theory with CCSD(T)/aug-cc-pVDZ single-point energy corrections. All relative energies are shown with harmonic zero-point energy corrections.

Because of the rich array of pathways through the substitution product region, a simple calculation of rates using, for example, transition state theory, is not sufficient for determining the time scales of these reactions. For such a system, exploration via AIMD is likely to yield greater insight into the conformationally complex pathways connecting the two IRCs shown in Fig. 1 due to the propensity for these systems to explore portions of the potential energy landscape away from the IRC.

It is not computationally feasible to run trajectories from initial reagents to the final products since the total simulation time required is prohibitively long. AIMD simulations were therefore performed such that the initial geometry was one of the two TS structures shown in Fig. 1. Thus, an understanding of the time scales involved in this process is formed from "stitching" together the process from multiple post-TS calculations. Initial velocities were sampled from a Boltzmann distribution at 300 K and run for a maximum of 10 ps. These initial conditions allow large regions of the potential energy surface to be efficiently sampled and thus provide new insights into reaction probabilities, time scales, and dissociation products.

Figure 2 illustrates a computed sequence of events, hence a reaction mechanism, for the halide substitution and hydrolysis reactions of N_2O_5 interacting with Cl^- and H_2O. As expected from the small barrier and proximity of the TS and minimum, halide substitution is a fast process, with an average time of 188 fs between minima, as shown in Fig. 2 (A to C). While there is not a substantial geometrical difference between intact $N_2O_5/Cl^-/H_2O$ and the TS structure (shown in Fig. 2, A and B), the O—N bond in N_2O_5 adjacent to the Cl^- is stretched to 1.80 Å at TS1 and relaxed to 1.62 Å at the minimum. The relaxation of this bond takes an average of 94 fs. Subsequent formation of the Cl—N bond in Fig. 2C also requires, on average, 94 fs. The mean time scales between local structures on the IRC is of the same order of magnitude as the Cl—N vibrational period of $ClNO_2$, which is ~90 fs (*38*). Thus, the reactive events are neither ballistic nor slow with respect to intramolecular vibrations.

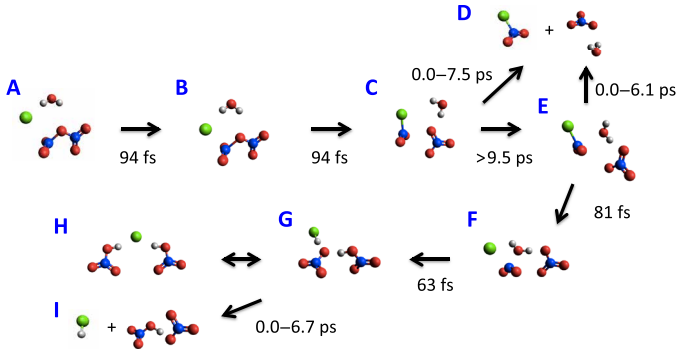

Fig. 2. Snapshots (A-I) of calculations of the reaction of N_2O_5 with Cl^- and H_2O.

As previously discussed, the ternary cluster $ClNO_2/H_2O/NO_3^-$ has a rich array of accessible configurations. Although direct observation of the hydrolysis from the initial $ClNO_2/H_2O/NO_3^-$ cluster is not observed in the calculations, 74% of trajectories that undergo substitution remain as an intact $ClNO_2/H_2O/NO_3^-$ cluster, while the other 26% exhibit dissociation into $ClNO_2$ and H_2O/NO_3^- products. The time scales of these dissociation processes are shown between Fig. 2 (C and D) (0.0 to 7.5 ps) and Fig. 2 (D and E) (0.0 to 6.1 ps), reflecting the time spent as an intact cluster entering from TS1 and TS2, respectively. Because most of the $ClNO_2/H_2O/NO_3^-$ clusters remain intact, the arrow between Figs. 2C and 2E, essentially the time spent between the two computed IRCs in Fig. 1, is set at a lower limit of 9.5 ps. The halide substitution cluster can, in theory, recross TS1 to form intact $N_2O_5/Cl^-/H_2O$, although this was not observed.

Lastly, time scales of the hydrolysis reaction are determined from trajectories initialized at TS2. All trajectories exhibiting hydrolysis form the ternary cluster $HCl/NO_3^-/HNO_3$, although the HCl proton moves freely between NO_3^- and Cl^-. HCl is efficiently ejected from this assembly to leave the NO_3^-/HNO_3 binary complex behind, with 67% of trajectories that undergo hydrolysis resulting in separation of HCl from the cluster. The time scales for this process range from 0.0 to 6.7 ps, where 0.0 ps indicates that HCl moves away from the cluster immediately after the reaction.

CONCLUSIONS

This theoretical study has identified mechanisms and time scales for the competing halide substitution and hydrolysis reactions of $N_2O_5/H_2O/Cl^-$, thus providing the first microscopic understanding of the key features underlying the reaction kinetics and pathways available for reactive uptake of N_2O_5 in the presence of aqueous Cl^-. Although the presence of Cl^- lowers the barrier to hydrolysis relative to the three-body $N_2O_5/(H_2O)_2$ reaction by ~15 kcal/mol, the third body adds significant entropic complexity. The predominance of halide substitution over hydrolysis is enabled by the proximity of the halide to N_2O_5 in the ternary cluster. In systems with larger water content, halide substitution is therefore expected to become less probable relative to hydrolysis. Qualitative insights into the behavior of these processes in more complicated systems such as larger clusters and macroscopic aerosols should nonetheless benefit from analysis of the local structures of the reagent molecules.

MATERIALS AND METHODS

Analysis

In analysis of bond formation and breaking in the molecular dynamics trajectories, various bond lengths were used as cutoffs. For formation of the Cl—N bond, a cutoff of 1.93 Å was used, which corresponds to the longest Cl—N bond length seen in the computed minima. The O—N bond distance cutoff in the hydrolysis reaction was set at 1.34 Å, the longer length observed in the hydrolysis products.

Theoretical calculations

All stationary geometries on the potential energy surface were optimized with the long-range corrected hybrid density functional ωB97X-D and basis set aug-cc-pVDZ (*39*–*41*). The diffuse functions included in the aug-cc-pVDZ basis set were needed to describe the diffuse nature of the negatively charged system. Zero-point energy corrections were made to the stationary point energies, computed using the harmonic approximation. IRCs were computed as described by Fukui (*34*).

To improve calculations of the relative energies of the structures in Fig. 1, single-point energy calculations were performed on top of the ωB97X-D–optimized geometries using coupled cluster theory with single, double, and perturbative triple excitations [CCSD(T)] paired with the aug-cc-pVDZ basis set (*40*–*43*).

AIMD calculations were performed at the ωB97X-D/aug-cc-pVDZ level of theory, as used for geometry optimizations and harmonic calculations. All calculations were initialized from each of the two TS structures shown in Fig. 1 (25 trajectories initialized from each geometry). Each trajectory was run with a time step of 0.2 fs for 10 ps or until the cluster dissociated. The relatively small time step was chosen to accurately describe hydrogen motion. All initial velocities were sampled from a Boltzmann distribution at 300 K. Fock extrapolation was performed with polynomial order 6 over 12 points (*44*, *45*). All calculations reported here were performed using Q-Chem (*46*) except for the CCSD(T)/aug-cc-pVDZ single-point energy calculations, which were performed in CFOUR (*47*).

SUPPLEMENTARY MATERIALS

Supplementary material for this article is available at http://advances.sciencemag.org/cgi/content/full/5/6/eaav6503/DC1

Table S1. Geometries optimized at the ωB97X-D/aug-cc-pVDZ level of theory, corresponding to those shown in Fig. 1 from left to right.

Table S2. Absolute and relative energies of eight structures shown in Fig. 1 calculated with ωB97X-D/aug cc-pVDZ and CCSD(T)/aug-cc-pVDZ.

REFERENCES AND NOTES

1. X. Tie, G. Brasseur, L. Emmons, L. Horowitz, D. Kinnison, Effects of aerosols on tropospheric oxidants: A global model study. *J. Geophys. Res. Atmos.* **106**, 22931–22964 (2001).
2. H. L. MacIntyre, M. J. Evans, Sensitivity of a global model to the uptake of N_2O_5 by tropospheric aerosol. *Atmos. Chem. Phys.* **10**, 7409–7414 (2010).
3. W. L. Chang, P. V. Bhave, S. S. Brown, N. Riemer, J. Stutz, D. Dabdub, Heterogeneous atmospheric chemistry, ambient measurements, and model calculations of N_2O_5: A review. *Aerosol Sci. Tech.* **45**, 665–695 (2011).
4. S. S. Brown, J. Stutz, Nighttime radical observations and chemistry. *Chem. Soc. Rev.* **41**, 6405–6447 (2012).
5. J. P. D. Abbatt, A. K. Y. Lee, J. A. Thornton, Quantifying trace gas uptake to tropospheric aerosol: Recent advances and remaining challenges. *Chem. Soc. Rev.* **41**, 6555–6581 (2012).
6. R. B. Gerber, M. E. Varner, A. D. Hammerich, S. Rilkonen, G. Murdachaew, D. Shemesh, B. J. Finlayson-Pitts, Computational studies of atmospherically-relevant chemical reactions in water clusters and on liquid water and ice surfaces. *Acc. Chem. Res.* **48**, 399–406 (2015).

7. E. E. McDuffie, D. L. Fibiger, W. P. Dubé, F. Lopez-Hilfiker, B. H. Lee, J. A. Thornton, V. Shah, L. Jaeglé, H. Guo, R. J. Weber, J. M. Reeves, A. J. Weinheimer, J. C. Schroder, P. Campuzano-Jost, J. L. Jimenez, J. E. Dibb, P. Veres, C. Ebben, T. L. Sparks, P. J. Wooldridge, R. C. Cohen, R. S. Hornbrook, E. C. Apel, T. Campos, S. R. Hall, K. Ullmann, S. S. Brown, Heterogeneous N_2O_5 uptake during winter: Aircraft measurements during the 2015 WINTER campaign and critical evaluation of current parameterizations. *J. Geophys. Res. Atmos.* **123**, 4345–4372 (2018).
8. F. J. Dentener, P. J. Crutzen, Reaction of N_2O_5 on tropospheric aerosols: Impact on the global distributions of NO_x, O_3, and OH. *J. Geophys. Res. Atmos.* **98**, 7149–7163 (1993).
9. M. J. Evans, D. J. Jacob, Impact of new laboratory studies of N_2O_5 hydrolysis on global model budgets of tropospheric nitrogen oxides, ozone, and OH. *Geophys. Res. Lett.* **32**, L09813 (2005).
10. S. S. Brown, T. B. Ryerson, A. G. Wollny, C. A. Brock, R. Peltier, A. P. Sullivan, R. J. Weber, W. P. Dubé, M. Trainer, J. F. Meagher, F. C. Fehsenfeld, A. R. Ravishankara, Variability in nocturnal nitrogen oxide processing and its role in regional air quality. *Science* **311**, 67–70 (2006).
11. C. J. Gaston, J. A. Thornton, Reacto-diffusive length of N_2O_5 in aqueous sulfate- and chloride-containing aerosol particles. *J. Phys. Chem. A* **120**, 1039–1045 (2016).
12. J. A. Logan, M. J. Prather, S. C. Wofsy, M. B. McElroy, Tropospheric chemistry: A global perspective. *J. Geophys. Res.* **86**, 7210–7254 (1981).
13. B. J. Finlayson-Pitts, M. J. Ezell, J. N. Pitts Jr., Formation of chemically active chlorine compounds by reactions of atmospheric NaCl particles with gaseous N_2O_5 and $ClONO_2$. *Nature* **337**, 241–244 (1989).
14. H. D. Osthoff, J. M. Roberts, A. R. Ravishankara, E. J. Williams, B. M. Lerner, R. Sommariva, T. S. Bates, D. Coffman, P. K. Quinn, J. E. Dibb, H. Stark, J. B. Burkholder, R. K. Talukdar, J. Meagher, F. C. Fehsenfeld, S. S. Brown, High levels of nitryl chloride in the polluted subtropical marine boundary layer. *Nat. Geosci.* **1**, 324–328 (2008).
15. J. M. Roberts, H. D. Osthoff, S. S. Brown, A. R. Ravishankara, D. Coffman, P. Quinn, T. Bates, Laboratory studies of products of N_2O_5 uptake on Cl^- containing substrates. *Geophys. Res. Lett.* **36**, L20808 (2009).
16. P. J. Kelleher, F. S. Menges, J. W. DePalma, J. K. Denton, M. A. Johnson, G. H. Weddle, B. Hirshberg, R. B. Gerber, Trapping and structural characterization of the $XNO_2{\cdot}NO_3^-$ (X = Cl, Br, I) exit channel complexes in the water-mediated X^- + N_2O_5 reactions with cryogenic vibrational spectroscopy. *J. Phys. Chem. Lett.* **8**, 4710–4715 (2017).
17. C. B. Faxon, D. T. Allen, Chlorine chemistry in urban atmospheres: A review. *Environ. Chem.* **10**, 221–233 (2013).
18. T. P. Riedel, G. M. Wolfe, K. T. Danas, J. B. Gilman, W. C. Kuster, D. M. Bon, A. Vlasenko, S.-M. Li, E. J. Williams, B. M. Lerner, P. R. Veres, J. M. Roberts, J. S. Holloway, B. Lefer, S. S. Brown, J. A. Thornton, An MCM modeling study of nitryl chloride ($ClNO_2$) impacts on oxidation, ozone production and nitrogen oxide partitioning in polluted continental outflow. *Atmos. Chem. Phys.* **14**, 3789–3800 (2014).
19. I. S. A. Isaksen, T. K. Berntsen, S. B. Dalsøren, K. Eleftheratos, Y. Orsolini, B. Rognerud, F. Stordal, O. A. Søvde, C. Zerefos, C. D. Holmes, Atmospheric ozone and methane in a changing climate. *Atmosphere* **5**, 518–535 (2014).
20. F. Schweitzer, P. Mirabel, C. George, Multiphase chemistry of N_2O_5, $ClNO_2$, and $BrNO_2$. *J. Phys. Chem. A* **102**, 3942–3952 (1998).
21. J. A. Thornton, J. P. D. Abbatt, N_2O_5 reaction on submicron sea salt aerosol: Kinetics, products, and the effect of surface active organics. *J. Phys. Chem. A* **109**, 10004–10012 (2005).
22. T. H. Bertram, J. A. Thornton, T. P. Riedel, An experimental technique for the direct measurement of N_2O_5 reactivity on ambient particles. *Atmos. Meas. Tech.* **2**, 231–242 (2009).
23. J. D. Raff, B. Njegic, W. L. Chang, M. S. Gordon, D. Dabdub, R. B. Gerber, B. J. Finlayson-Pitts, Chlorine activation indoors and outdoors via surface-mediated reactions of nitrogen oxides with hydrogen chloride. *Proc. Natl. Acad. Sci. U.S.A.* **106**, 13647–13654 (2009).
24. W. Behnke, C. George, V. Scheer, C. Zetzsch, Production and decay of $ClNO_2$ from the reaction of gaseous N_2O_5 with NaCl solution: Bulk and aerosol experiments. *J. Geophys. Res. Atmos.* **102**, 3795–3804 (1997).
25. T. H. Bertram, J. A. Thornton, Toward a general parameterization of N_2O_5 reactivity on aqueous particles: The competing effects of particle liquid water, nitrate and chloride. *Atmos. Chem. Phys.* **9**, 8351–8363 (2009).
26. D. Hanway, F.-M. Tao, A density functional theory and ab initio study of the hydrolysis of dinitrogen pentoxide. *Chem. Phys. Lett.* **285**, 459–466 (1998).
27. J. A. Snyder, D. Hanway, J. Mendez, A. J. Jamka, F.-M. Tao, A density functional theory study of the gas-phase hydrolysis of dinitrogen pentoxide. *J. Phys. Chem. A* **103**, 9355–9358 (1999).
28. R. Bianco, J. T. Hynes, Theoretical studies of heterogeneous reaction mechanisms relevant for stratospheric ozone depletion. *Int. J. Quantum Chem.* **75**, 683–692 (1999).
29. J. P. McNamara, I. H. Hillier, Structure and reactivity of dinitrogen pentoxide in small water clusters studied by electronic structure calculations. *J. Phys. Chem. A* **104**, 5307–5319 (2000).
30. A. F. Voegele, C. S. Tautermann, T. Loerting, K. R. Liedl, Toward elimination of discrepancies between theory and experiment: The gas-phase reaction of N_2O_5 with H_2O. *Phys. Chem. Chem. Phys.* **5**, 487–495 (2003).
31. I. M. Alecu, P. Marshall, Computational study of the thermochemistry of N_2O_5 and the kinetics of the reaction $N_2O_5 + H_2O \rightarrow 2\ HNO_3$. *J. Phys. Chem. A* **118**, 11405–11416 (2014).
32. J. P. McNamara, I. H. Hillier, Exploration of the atmospheric reactivity of N_2O_5 and HCl in small water clusters using electronic structure methods. *Phys. Chem. Chem. Phys.* **2**, 2503–2509 (2000).
33. A. D. Hammerich, B. J. Finlayson-Pitts, R. B. Gerber, Mechanism for formation of atmospheric Cl atom precursors in the reaction of dinitrogen oxides with HCl/Cl^- on aqueous films. *Phys. Chem. Chem. Phys.* **17**, 19360–19370 (2015).
34. K. Fukui, Formulation of the reaction coordinate. *J. Phys. Chem.* **74**, 4161–4163 (1970).
35. R. V. Martin, D. J. Jacob, R. M. Yantosca, M. Chin, P. Ginoux, Global and regional decreases in tropospheric oxidants from photochemical effects of aerosols. *J. Geophys. Res. Atmos.* **108**, 4097 (2003).
36. H. Liao, P. J. Adams, S. H. Chung, J. H. Seinfeld, L. J. Mickley, D. J. Jacob, Interactions between tropospheric chemistry and aerosols in a unified general circulation model. *J. Geophys. Res.* **108**, AAC 1-1–AAC 1-23 (2003).
37. J. A. Thornton, C. F. Braban, J. P. D. Abbatt, N_2O_5 hydrolysis on sub-micron organic aerosols: The effect of relative humidity, particle phase, and particle size. *Phys. Chem. Chem. Phys.* **5**, 4593–4603 (2003).
38. J. R. Durig, Y. H. Kim, G. A. Guirgis, J. K. McDonald, FT-Raman and infrared spectra, r_0 structural parameters, ab initio calculations and vibrational assignment for nitryl chloride. *Spectrochim. Acta A Mol. Spectrosc.* **50**, 463–472 (1994).
39. J.-D. Chai, M. Head-Gordon, Long-range corrected hybrid density functionals with damped atom–atom dispersion corrections. *Phys. Chem. Chem. Phys.* **10**, 6615–6620 (2008).
40. R. A. Kendall, T. H. Dunning Jr., R. J. Harrison, Electron affinities of the first-row atoms revisited. Systematic basis sets and wave functions. *J. Chem. Phys.* **96**, 6796–6806 (1992).
41. D. E. Woon, T. H. Dunning Jr., Gaussian basis sets for use in correlated molecular calculations. III. The atoms aluminum through argon. *J. Chem. Phys.* **98**, 1358–1371 (1993).
42. K. Raghavachari, G. W. Trucks, J. A. Pople, M. Head-Gordon, A fifth-order perturbation comparison of electron correlation theories. *Chem. Phys. Lett.* **157**, 479–483 (1989).
43. R. J. Bartlett, J. D. Watts, S. A. Kucharski, J. Noga, Non-iterative fifth-order triple and quadruple excitation energy corrections in correlated methods. *Chem. Phys. Lett.* **165**, 513–522 (1990).
44. J. M. Herbert, M. Head-Gordon, Accelerated, energy-conserving Born–Oppenheimer molecular dynamics via Fock matrix extrapolation. *Phys. Chem. Chem. Phys.* **7**, 3269–3275 (2005).
45. P. Pulay, G. Fogarasi, Fock matrix dynamics. *Chem. Phys. Lett.* **386**, 272–278 (2004).
46. Y. Shao, Z. Gan, E. Epifanovsky, A. T. B. Gilbert, M. Wormit, J. Kussmann, A. W. Lange, A. Behn, J. Deng, X. Feng, D. Ghosh, M. Goldey, P. R. Horn, L. D. Jacobson, I. Kaliman, R. Z. Khaliullin, T. Kuś, A. Landau, J. Liu, E. I. Proynov, Y. M. Rhee, R. M. Richard, M. A. Rohrdanz, R. P. Steele, E. J. Sundstrom, H. L. Woodcock III, P. M. Zimmerman, D. Zuev, B. Albrecht, E. Alguire, B. Austin, G. J. O. Beran, Y. A. Bernard, E. Berquist, K. Brandhorst, K. B. Bravaya, S. T. Brown, D. Casanova, C.-M. Chang, Y. Chen, S. H. Chien, K. D. Closser, D. L. Crittenden, M. Diedenhofen, R. A. DiStasio Jr., H. Do, A. D. Dutoi, R. G. Edgar, S. Fatehi, L. Fusti-Molnar, A. Ghysels, A. Golubeva-Zadorozhnaya, J. Gomes, M. W. D. Hanson-Heine, P. H. P. Harbach, A. W. Hauser, E. G. Hohenstein, Z. C. Holden, T.-C. Jagau, H. Ji, B. Kaduk, K. Khistyaev, J. Kim, J. Kim, R. A. King, P. Klunzinger, D. Kosenkov, T. Kowalczyk, C. M. Krauter, K. U. Lao, A. D. Laurent, K. V. Lawler, S. V. Levchenko, C. Y. Lin, F. Liu, E. Livshits, R. C. Lochan, A. Luenser, P. Manohar, S. F. Manzer, S.-P. Mao, N. Mardirossian, A. V. Marenich, S. A. Maurer, N. J. Mayhall, E. Neuscamman, C. M. Oana, R. Olivares-Amaya, D. P. O'Neill, J. A. Parkhill, T. M. Perrine, R. Peverati, A. Prociuk, D. R. Rehn, E. Rosta, N. J. Russ, S. M. Sharada, S. Sharmaa, D. W. Small, A. Sodt, T. Stein, D. Stück, Y.-C. Su, A. J. W. Thom, T. Tsuchimochi, V. Vanovschi, L. Vogt, O. Vydrov, T. Wang, M. A. Watson, J. Wenzel, A. White, C. F. Williams, J. Yang, S. Yeganeh, S. R. Yost, Z.-Q. You, I. Y. Zhang, X. Zhang, Y. Zhao, B. R. Brooks, G. K. L. Chan, D. M. Chipman, C. J. Cramer, W. A. Goddard III, M. S. Gordon, W. J. Hehre, A. Klamt, H. F. Schaefer III, M. W. Schmidt, C. D. Sherrill, D. G. Truhlar, A. Warshel, X. Xu, A. Aspuru-Guzik, R. Baer, A. T. Bell, N. A. Besley, J.-D. Chai, A. Dreuw, B. D. Dunietz, T. R. Furlani, S. R. Gwaltney, C.-P. Hsu, Y. Jung, J. Kong, D. S. Lambrecht, W. Liang, C. Ochsenfeld, V. A. Rassolov, L. V. Slipchenko, J. E. Subotnik, T. Van Voorhis, J. M. Herbert, A. I. Krylov, P. M. W. Gill, M. Head-Gordon, Advances in molecular quantum chemistry contained in the Q-Chem 4 program package. *Mol. Phys.* **113**, 184–215 (2015).
47. CFOUR, Coupled-Cluster techniques for Computational Chemistry, a quantum-chemical program package by J.F. Stanton, J. Gauss, L. Cheng, M.E. Harding, D.A. Matthews, P.G. Szalay with contributions from A.A. Auer, R.J. Bartlett, U. Benedikt, C. Berger, D.E. Bernholdt, Y.J. Bomble, O. Christiansen, F. Engel, R. Faber, M. Heckert, O. Heun, M. Hilgenberg, C. Huber, T.-C. Jagau, D. Jonsson, J. Jusélius, T. Kirsch, K. Klein, W.J. Lauderdale, F. Lipparini, T. Metzroth, L.A. Mück, D.P. O'Neill, D.R. Price, E. Prochnow,

C. Puzzarini, K. Ruud, F. Schiffmann, W. Schwalbach, C. Simmons, S. Stopkowicz, A. Tajti, J. Vázquez, F. Wang, J.D. Watts and the integral packages *MOLECULE* (J. Almlöf and P.R. Taylor), *PROPS* (P.R. Taylor), *ABACUS* (T. Helgaker, H.J. Aa. Jensen, P. Jørgensen, and J. Olsen), and ECP routines by A. V. Mitin and C. van Wüllen. For the current version, see www.cfour.de.

Acknowledgments
Funding: This work was supported by the U.S. National Science Foundation Center for Aerosol Impacts on Chemistry of the Environment (NSF-CAICE), CHE-1801971, XSEDE allocation TG-CHE17006, and Zuckerman STEM Leadership Program. **Author contributions:** L.M.M. performed the calculations and analysis and wrote the majority of the manuscript. M.A.J. provided insights into the connection to cluster studies. R.B.G. proposed the model system and contributed to the analysis. All authors contributed to the interpretation of the results.

Competing interests: The authors declare that they have no competing interests. **Data and materials availability:** Data needed to evaluate the conclusions in the paper can be accessed from the NSF-CAICE Data Repository (doi:10.6075/J0S75DPT). All data needed to evaluate the conclusions in the paper are present in the paper and/or the Supplementary Materials. Additional data related to this paper may be requested from the authors.

Submitted 7 October 2018
Accepted 2 May 2019
Published 5 June 2019
10.1126/sciadv.aav6503

Citation: L. M. McCaslin, M. A. Johnson, R. B. Gerber, Mechanisms and competition of halide substitution and hydrolysis in reactions of N_2O_5 with seawater. *Sci. Adv.* **5**, eaav6503 (2019).